FRACTURE ENERGY OF SPRUCE WOOD AFTER DIFFERENT DRYING PROCEDURES[1]

Stefanie E. Stanzl-Tschegg

Professor
Institut für Meteorologie und Physik, Universität für Bodenkultur
Türkenschanzstraße 18, A-1180 Vienna, Austria

Elmar K. Tschegg

Professor
Institut für Technische und Angewandte Physik, Technische Universität
Karlsplatz 13, A-1040 Vienna, Austria

and

Alfred Teischinger

Head
Versuchsanstalt für Holzindustrie, HTBLuVA Mödling/Abt. Holztechnik
Technikerstraße 1-5, A-2340 Mödling, Austria

(Received October 1993)

ABSTRACT

The effects of different wood drying procedures, of felling time (winter and summer), and of compass orientation within one tree (north and south side) on the fracture properties of spruce wood have been studied. A most useful parameter to characterize the fracture behavior, the specific fracture energy G_f, has been determined with a new splitting method. High-temperature (100–110 C) drying renders the lowest specific fracture energy (G_f) and fracture toughness (K_{IC}) values in comparison with 20 C fresh air, 50–60 C (kiln)-drying and prefreezing (−20 C), and air-drying. Prefreezing to −20 C before air-drying provides similar values as 20 C and similar or slightly higher values as 50 C drying. Effects of felling time and of compass orientation could not be detected unambiguously.

Keywords: Wood drying, fracture energy, splitting force, orientation influence, felling time, microstructure.

INTRODUCTION

Wood drying is an extremely complex process in which a great number of physical and chemical actions within the wood are combined. The quality of the wood during the drying process is to be maintained or improved. Though practical wood engineering demands a certain quality of dried wood, generally valid standards have not been established so far in Europe (Welling and Sales 1992). Moreover, the various physical and chemical processes, especially their combined action during the drying process, have not been studied enough in order to use them for the dry-kiln control system (Kayihan et al. 1989).

It has to be assumed that the quality of the dried wood is influenced not only by the drying process itself but also by a number of different factors, e.g., the conditions previous to cutting or the time of felling itself. The possible influences of felling time in connection with the drying process have so far been discussed only vaguely (Teischinger 1992).

An extensive literature review on the influence of drying processes on several wood properties is given by Teischinger (1991, 1992). Among other things, the physical properties, like equilibrium moisture content, swelling and

[1] Dedicated to the 60th birthday of Prof. Dr. Gisbert Greshake, Universität Freiburg, Germany.

Wood and Fiber Science, 26(4), 1994, pp. 467–478

shrinkage and color changes, as well as the resulting mechanical properties like bending or tensile strength and modulus of elasticity, have been studied. It has been shown that strength properties were in some cases influenced by increased drying temperatures (80–115 C), owing to changed sorption behavior. A decrease in the strength properties has been reported in some cases, whereas no unique result has been obtained by many other authors. Differences in shrinkage during different drying procedures and the resulting residual drying stresses play the most important part and thus influence wood quality.

A straightforward means to characterize the influence of residual drying stresses is to investigate fracture behavior after a defined drying procedure. Schniewind and Pozniak (1971), as well as Ewing and Williams (1979), performed such studies on Douglas-fir wood and Scots pine, respectively, using fracture mechanics principles.

Another possibility of investigating the influence of drying procedures on wood properties is to study the chemical processes taking place during drying and the resulting changes in chemical properties. Such studies have been reviewed and also performed by Hinterstoisser et al. (1992).

In order to study the fracture properties of wood, various attempts have been made to use linear elastic fracture mechanics (LEFM) principles. As a characteristic measuring parameter, stress intensity factor and fracture toughness have been tested and used in most studies, though wood is a highly oriented and anisotropic material. Important contributions to this subject have been made by Schniewind and Pozniak (1971), who studied the influence of anisotropy owing to orientation on fracture toughness with different types of specimens and who also showed that residual drying stresses largely influence the fracture toughness. Barrett and Foschi (1977) studied Mode II crack propagation in longitudinal orientation; and Barrett (1976) treated the effect of specimen thickness on the fracture toughness, K_{IC}, and the increase of K_{IC} with increasing strain rate and its dependence on specimen orientation. Boatright and Garrett (1983) correlated macroscopic fracture properties with micromechanical features of wood. Valentin and Adjanohoun (1992) have dealt with the question of using isotropic fracture mechanics for wood as an orthotropic material and have critically discussed the applicability of fracture mechanics on wood crack propagation for different orientations. Triboulet et al. (1984) proved the validity of fracture mechanical approaches based on the assumption of an elastic and orthotropic material by finite element calculations. A correlation between ultimate tangential tensile stress and fracture toughness is described by Petterson and Bodig (1983). Patton-Mallory and Cramer (1987), who give an extensive literature review on fracture mechanical treatment of wood, point out the possibility of predicting fracture loads of wood components that contain stress concentrations caused by discontinuities like knots, notches, splits, etc., on the basis of fracture mechanical considerations.

Owing to the complex structure of wood, however, the question arises whether stress intensity factor and fracture toughness are satisfying parameters to characterize its fracture properties. For example, it was shown by Tschegg and Stanzl (1991), that in other inhomogeneous materials, like concrete or asphalt aggregate mixtures, the maximum load values did not describe fracture behavior adequately. Different bonds of concrete, for example, displayed identical maximum load values though their fracture behavior was completely different, one being brittle and the other ductile. Similarly, it might be expected that the fracture toughness that is adequate to describe linear elastic and isotropic materials is not the most appropriate value to describe a fibrous material like wood. One might expect, for example, that wood fibers cause "fiber bridging" (an already formed crack is bridged by fibers so that final fracturing is delayed) and crack closure as a consequence, so that LEFM parameters do not really characterize this material.

On the other hand, it could be shown that the specific fracture energy, G_f, which is determined by the so-called softening behavior in the load displacement curve, is much more appropriate to characterize the fracturing behavior of inhomogeneous materials (Tschegg and Stanzl 1991). The first to study the fracture energy as a material parameter for wood was Porter (1964). Schniewind et al. (1982) critically compared this parameter with fracture toughness values and studied influences of moisture content, temperature, and specific gravity. In a more recent work, Boström (1992) and Petersson (1992) applied the fracture energy concept and the fictitious crack model (Hillerborg 1991) in studies of the fracture properties of wood.

In this paper, fracture energy and fracture toughness have been determined in order to study the influence of different drying procedures on the fracture properties of spruce wood. A new and simple specimen shape and testing procedure has been used for these measurements, which was developed and used by Tschegg (1986) to characterize the fracturing of concrete, asphalt aggregate mixtures, and other heterogeneous materials. It was also used later by Navi (1992).

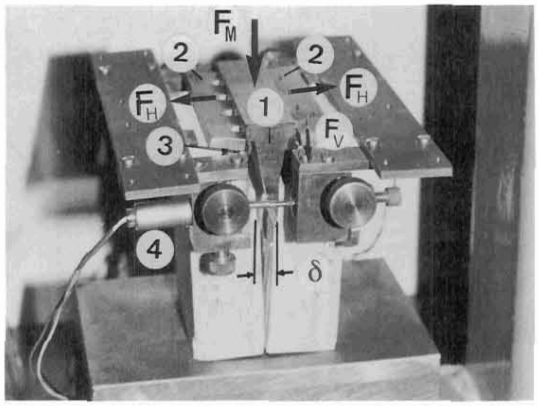

FIG. 1. Cubic wood specimens with measuring equipment: 1: wedge, 2: load transmission pieces, 3: roll bodies, 4: LVDT. F_M = force acting on the wedge, F_H = horizontal force component, F_V = vertical force component, δ = COD.

TESTING PROCEDURE

Specimens were rectangular blocks with side lengths of 80 × 80 × 100 mm (shown in Fig. 1, together with the testing fixture). This specimen size was found in pretests (details in Stanzl-Tschegg et al. 1993) to give useful values of the wood properties of trees having a diameter of approximately 30–40 cm. Grooves, and on the bottom of these, 15-mm-deep starter notches, were introduced with a saw. In order to obtain sharp and reproducible starter notches, additional 0.5-mm-deep cuts were finally made with a razor blade (tip radius <5 μm) (Fig. 2).

For the splitting test, a specimen is placed on a narrow linear support area that is oriented parallel to the groove. The load is transmitted from a stiff spindle machine to a slender wedge (wedge angle 15°), which is pressed in between two load transmission pieces placed on the rectangular groove. In order to suppress friction to a negligible value, steel rolls are inserted between the load transmission pieces and the wedge. The main part of the force acts horizontally as a splitting force (F_H), whereas the vertical component (F_V) is small enough to be ignored.

In order to detect the complete load displacement curve, splitting must be performed during stable crack growth until complete separation of the specimen takes place. For this purpose, the equipment described above (i.e., wedge, loading system, and spindle machine) is optimal as it is very stiff. The velocity of load application was 0.1 mm/min in all tests.

The displacements δ are measured in the line of application of the force, F_H, with two LVDTs fixed at the front and the rear surface of the specimen by a frame and screws. The force acting on the wedge is measured by a load cell between testing machine and wedge. Force F_M and displacement δ are registered by an X-Y1-Y2 recorder or a datalogger. The horizontal force component, F_H, is easily obtained from F_M with the aid of the wedge angle.

MATERIAL

Test material was wood from spruce trees, cut about 60 km south of Vienna (Rosalia Lehrforst of the University of Agriculture). Fifteen trees were cut on 17 July 1990, to characterize a "summer-cut," and seventeen were

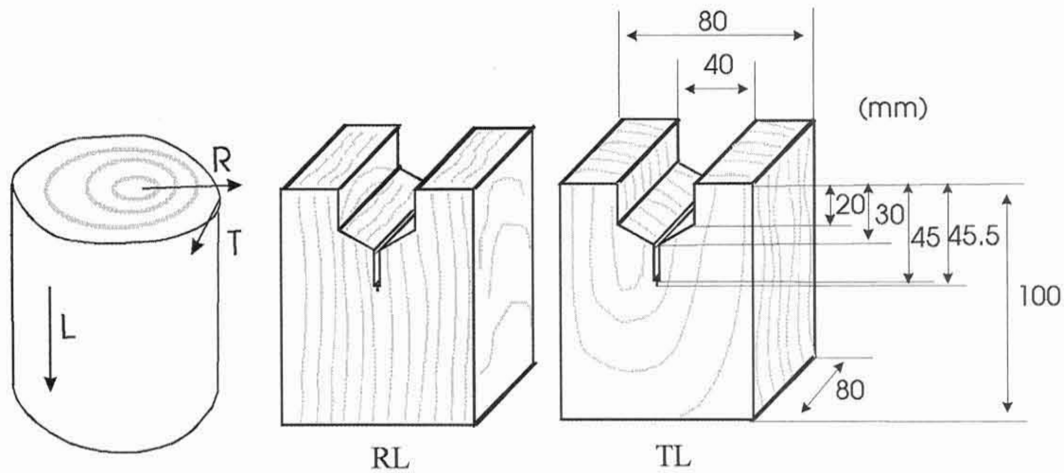

FIG. 2. Longitudinal (L), radial (R) and tangential (T) orientations in a tree trunk and in cubic specimens; dimensions of tested specimens.

cut in the same place on 22 January 1991. However, this was probably not quite a typical "winter-cut" since it had been untypically warm for about 4 weeks before felling time. Cubes 15 × 15 cm were prepared from each tree, with one cube of timber coming from the north and one from the south side of the tree, shown by Teischinger (1992). Matching specimens were prepared for measuring density, swelling, and shrinkage, as well as bending strength and modulus of elasticity (Teischinger 1992). The density values were obtained according to the standard DIN 52182 (1976) and did not differ significantly for the different drying treatments. Mean values and standard deviations are listed in Table 1. In addition, chemical measurements of extractable carbohydrates and reducing substances were performed (Hinterstoisser et al. 1992).

TABLE 1. *Density values[1] (means and standard deviations) of spruce wood after different drying procedures.*

Drying process	Winter cut $\bar{x}$	Winter cut σ	Summer cut $\bar{x}$	Summer cut σ
Prefreeze	0.52	0.04	0.47	0.07
Air drying	0.52	0.05	0.52	0.05
Kiln drying	0.51	0.05	0.51	0.04
High temp.	0.50	0.05	0.51	0.05

[1] Oven-dry density according to DIN 52182, in g/cm^3.

After machining, the specimens were dried by using four different drying procedures:

No. 1. prefreezing at −20 C one month, then air-drying as for No. 2
No. 2. air-drying at 20 C under shelter for several months
No. 3. kiln-drying at 50–60 C for 650 hours
No. 4. high-temperature drying at 100–110 C for 145 hours.

After drying to a final moisture content (MC) of about 12–13%, the specimens were conditioned at 20 C and 65% relative humidity to almost equilibrium moisture content. Then the final shapes (80- × 80- × 100-mm rectangular blocks with grooves and notches) were machined, and the specimens were stored at 20 C and 65% relative humidity until testing. Two directions were chosen for introducing grooves and notches: one was in the T direction so that fracturing took place in the RL orientation (R: direction of horizontal forces acting, L: crack propagation direction) and the second was in the R direction so that TL was the fracture orientation (with T the direction of horizontal forces, Fig. 2).

EXPERIMENTAL RESULTS

The fracture energies (or crack resistance values) W were determined from the measured

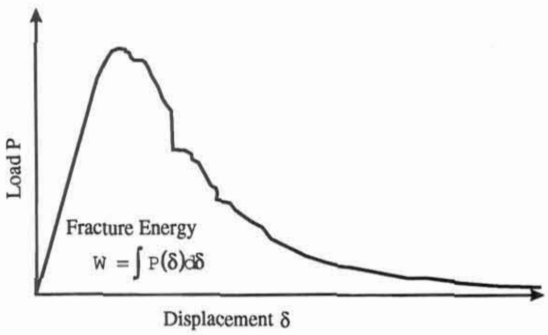

FIG. 3. Typical load-displacement curve and fracture energy, W.

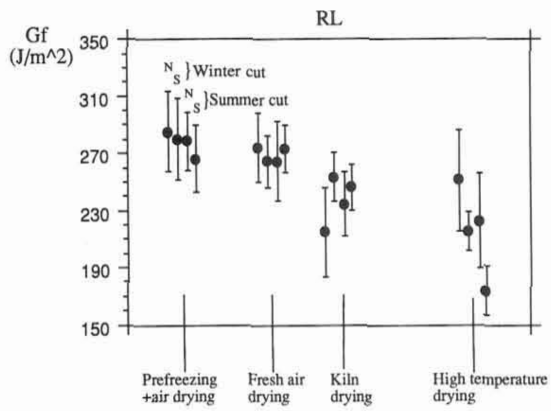

FIG. 4. Influence of different drying procedures on specific fracture energy, G_f, in the RL orientation.

load displacement curves (after electronic smoothing) by integrating the area under these curves, where the load P is plotted vs. the displacement δ (Fig. 3). The specific fracture energies (G_f) were obtained by dividing the results by the fracture area values (normal projection). In addition the fracture toughness values (K_{IC}) were obtained from the maximum splitting forces using a FE program and assuming small anisotropic deformation as described in detail in another study (Stanzl-Tschegg et al. 1993).

Table 2 shows the mean values and standard deviations of G_f and K_{IC} for each drying treatment, both orientations, both compass orientations, and both felling times. Approximately fifteen measurements were performed and evaluated for each test series.

In Fig. 4 the influence of the drying temperature on the G_f values is shown for the RL orientation (load direction R, crack propagation direction L, fracture area RL). The data

TABLE 2. *Influence of drying procedure, orientation, felling time and compass orientation on G_F and K_{IC}.*

Drying process	Winter cut north side	Winter cut south side	Summer cut north side	Summer cut south side
	G_F (J/m^2) in RL orientation			
Prefreezing + air-drying	284 ± 28	228 ± 28	281 ± 19	268 ± 23
Fresh air-drying	272 ± 24	273 ± 26	280 ± 36	267 ± 22
Kiln-drying	214 ± 31	259 ± 21	249 ± 31	256 ± 21
High-temperature drying	253 ± 35	222 ± 37	248 ± 52	185 ± 45
	K_{IC} (kPa$\sqrt{m}$) in RL orientation			
Prefreezing + air-drying	526 ± 30	547 ± 39	590 ± 24	564 ± 34
Fresh air-drying	517 ± 23	517 ± 40	692 ± 61	597 ± 45
Kiln-drying	520 ± 22	529 ± 37	601 ± 34	530 ± 35
High-temperature drying	466 ± 31	464 ± 20	529 ± 75	475 ± 68
	G_F (J/m^2) in TL orientation			
Prefreezing + air-drying	202 ± 29	246 ± 100	223 ± 27	214 ± 23
Fresh air-drying	220 ± 37	207 ± 25	268 ± 30	226 ± 40
Kiln-drying	272 ± 19	170 ± 39	227 ± 31	203 ± 35
High-temperature-drying	291 ± 32	257 ± 23	315 ± 39	208 ± 24
	K_{IC} (kPa$\sqrt{m}$) in TL orientation			
Prefreezing + air-drying	486 ± 27	471 ± 23	456 ± 33	467 ± 30
Fresh air-drying	480 ± 27	449 ± 33	657 ± 52	519 ± 47
Kiln-drying	487 ± 20	445 ± 46	546 ± 49	519 ± 38
High-temperature drying	426 ± 21	418 ± 34	526 ± 76	415 ± 45

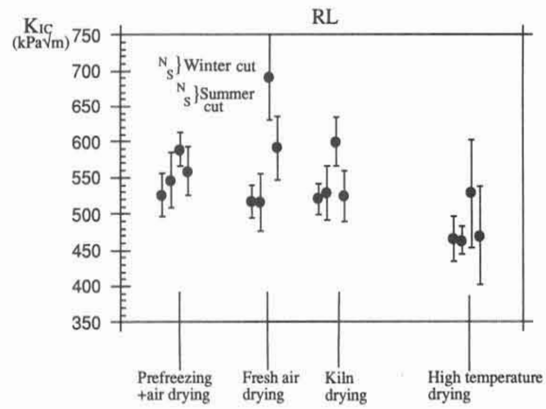

FIG. 5. Influence of different drying procedures on critical fracture toughness, K_{IC}, in the RL orientation.

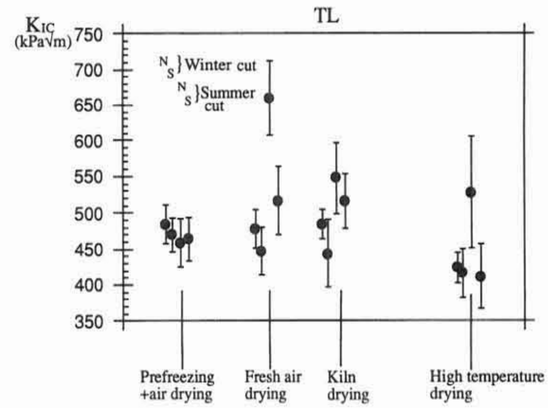

FIG. 7. Influence of drying procedure on critical fracture toughness, K_{IC}, in the TL orientation.

points are mean values of approximately fifteen measurements for each drying temperature, and the standard deviations are also plotted. The data points termed "winter" refer to felling in winter, and the data points termed "summer" refer to summer felling. The data points termed "N" characterize the north, and the data points termed "S" characterize the south side of the trees.

The diagrams show great scattering; however, they provide important results:

1. The specific fracture energies, G_f, are similar for winter and summer felling.
2. The G_f values are also similar for the north and south sides of the trees.
3. The G_f values decrease with increasing drying temperature up to 50–60 C and are remarkably smaller for 100–110 C drying, though the increased value for the wintercut of the north side does not follow this tendency at a drying temperature of 100–110 C. This result, however, does not seem typical; it is probably caused by a geometric effect. It was observed that in most of these specimens the following behavior was especially well pronounced: the crack did not stay within one TL plane during propagation but changed to another.

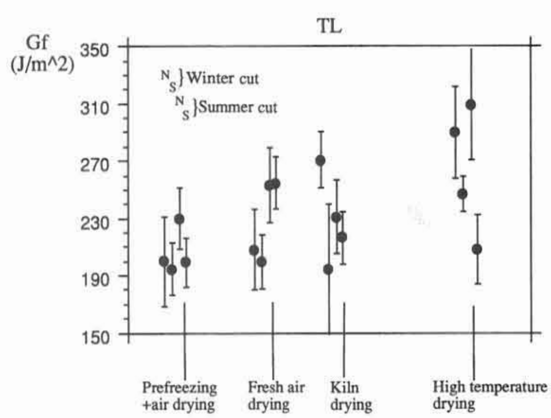

FIG. 6. Influence of drying procedure on specific fracture energy, G_f, in the TL orientation.

In Fig. 5 the fracture toughness values, K_{IC}, are plotted versus the drying temperature for the RL orientation and the following is shown:

1. The K_{IC} values seem to be higher for trees cut in summer, but the scattering of the data is so great that this result is rather questionable.
2. The K_{IC} results are similar for the north and south sides.
3. The K_{IC} values of trees cut in winter are approximately the same for prefreezing plus air-drying, for 20 C and 50–60 C drying, while for summer felling K_{IC} is lower after prefreezing plus air-drying.
4. A 20 to 30% decrease of the K_{IC} values is very evident after high-temperature drying.

Figure 6 shows the influence of drying temperature on the specific fracture energy, G_f, when splitting is performed in the TL orientation. The figure shows:

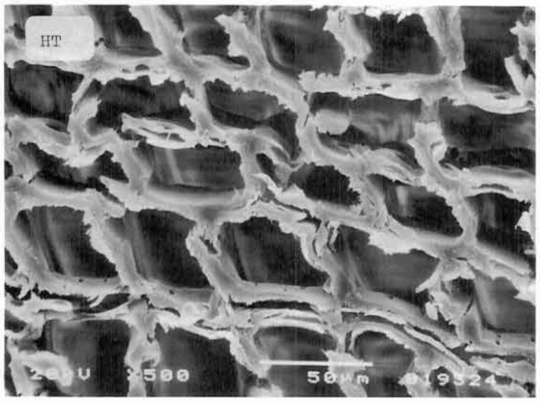

FIG. 8. Microstructure after 100–110 C drying (SEM view of cross section): Longitudinal cracks within middle lamellas (intercellular) and longitudinal cracks through cell walls (intracellular); distorted cell shapes.

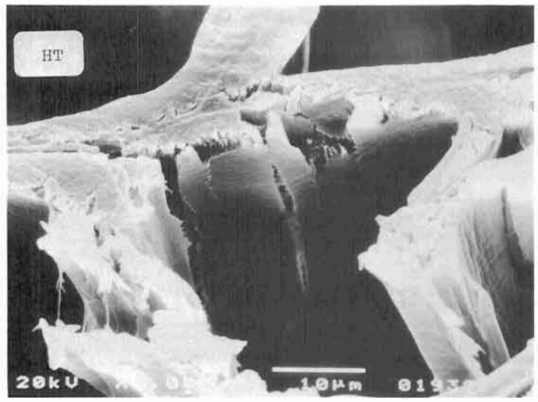

FIG. 9. Cracks visible in tertiary wall in specimen after high-temperature drying.

1. For this orientation, scattering is more pronounced than for the RL orientation. Therefore the results probably do not show a similarly clear tendency as for the RL orientation.
2. Besides this result, no pronounced difference between the drying procedures of prefreezing, air-drying, and kiln-drying is evident.
3. In addition, it seems that the fracture energy is higher after high-temperature drying. This effect is shown for wood cut in winter in both compass orientations and for wood cut in summer on the north side.

In Fig. 7 the K_{IC} values are plotted for the TL orientation. Similar tendencies as for the RL orientation are observed.

Summarizing the K_{IC} results, more scattering for wood after felling in summer than in winter is obtained. In addition, slightly higher K_{IC} values for the RL than for the TL orientation and almost no influence of the compass direction (north or south side) are visible. The drying procedure, up to a drying temperature of 50–60 C, does not change the K_{IC} values notably. Specimens that were dried at 100–110 C, however, are characterized by lower K_{IC} values in all cases.

In order to interpret the observed influences of drying temperature on fracture energy and fracture toughness, SEM studies of the microstructure were performed. The main result is that after 100–110 C drying, almost all middle lamellas were cracked parallel to their wall direction (longitudinal orientation in the tree). In addition, numerous cell walls were cracked perpendicular to their thickness direction, parallel to the longitudinal orientation of the tree. Furthermore, the cell shapes were obviously changed by the high-temperature drying procedure. In Fig. 9 cracks in the tertiary wall of a high-temperature dried specimen are visible.

The prefreezing plus air-drying procedure results in fewer cracks within the middle lamellas and also fewer orthogonal cracks in the cell walls (Fig. 10). No distortion of the cell shapes has taken place. Figure 11 shows the cracks in a longitudinal cut (TL section) of a

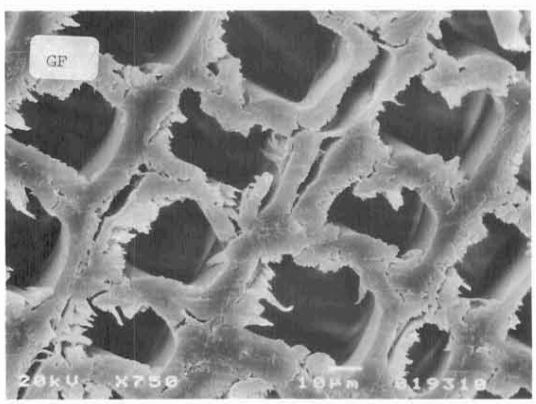

FIG. 10. Prefreezing (−20 C) + natural drying (20 C): fewer cracks and no distortion of cells.

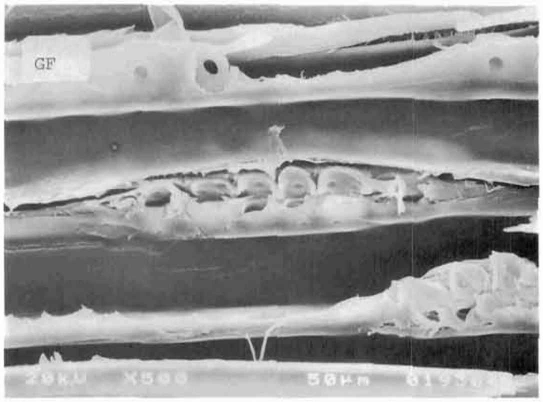

FIG. 11. Longitudinal cross section of a specimen after prefreezing + natural drying: Inter- and intracellular cracks.

prefrozen + fresh air-dried specimen. Intercellular cracking and a ray are visible.

Drying at 50–60 C is characterized by eventual, less extensive cracking within the middle lamellas and by fewer cracks perpendicular to the cell walls than drying at −20 C or 100–110 C. 20 C air-drying results in few intercellular and almost no cracks within the cell walls.

The types of cracks shown in the photographs of Figs. 8–11 are drawn schematically in Fig. 12.

DISCUSSION

The most obvious and most important result of this paper is the lower values of the specific fracture energy, G_f, and of the fracture toughness K_{IC} after high-temperature drying in comparison with natural, kiln and prefreezing + natural drying.

The SEM observations may partly explain this result: Numerous cracks on a microscopic scale (in the middle lamellas of the longitudinal tracheids and cell walls) have obviously led to a weakening of the structure. The main reason for the extensive microcracking observed may be the high velocity of drying and thus water extraction at 100–110 C. Air-drying (20 C) is slowest so that reduced or almost zero microcracking could be observed in the SEM. Kiln-drying (50–60 C) is slower than high-temperature drying, but faster than 20 C. The observed number of microstructural cracks reflects this behavior. The higher number of microstructural cracks in prefrozen specimens

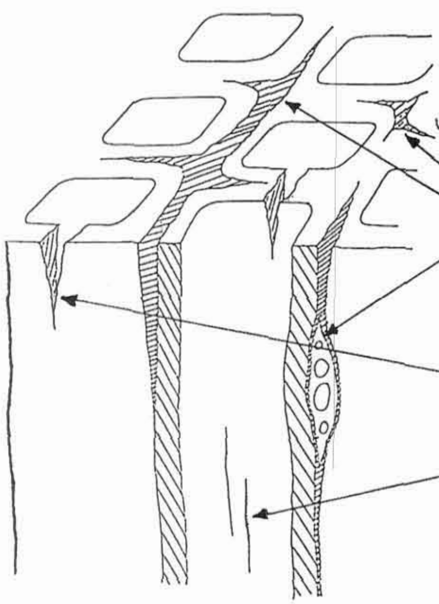

FIG. 12. Schematic presentation of microstructural cracking as seen in Figs. 8–11.

does not fully coincide with the fracture energy and fracture toughness results that were higher or at least similarly high for 50 C (and 20 C) drying.

The G_f, K_{IC}, and SEM results of this paper are interesting in comparison with the Hinterstoisser et al. (1992) chemical studies. They found that 20 C and 50–60 C dried specimens contained similar values of water-extractable carbohydrates, whereas high-temperature dried specimens showed up to four times higher levels, and prefrozen specimens the lowest values. The measured extractables were monosaccharides, which are the main constituents of the hemicellulosic part of the cell wall. They act as a kind of coupling agent between cellulose and lignin and are therefore very important for the strength of wood. The influence of drying temperature on the G_f and K_{IC} values as described above and also the SEM findings on the number of microstructural cracks in 20 C, 50–60 C and 100–110 C dried specimens parallel the results of Hinterstoisser et al. (1992). These parallels point to the importance of hemicelluloses for the strength of wood. However, precracking of the cell walls on a microscopic scale obviously is of secondary importance. Closer studies are necessary in order to understand the mechanisms and effects of prefreezing on the fracture behavior of wood.

Another point to be discussed in this study is the fact that the G_f and K_{IC} measurements reveal essentially similar results, but that scatter of the G_f results is in part greater. The second result is not surprising if one considers that measuring G_f values includes crack propagation. This is strongly influenced by the crack path, which is different in different pieces of wood. Therefore, different energies are consumed to propagate these cracks.

One reason for differing crack paths is the different curvatures of annual rings. These curvatures are different for each tested specimen, though we took care to place the notch into similarly curved annual rings in all specimens. The rather large specimens used in this study, however, are responsible for the fact that the angle between load axis and year ring is not 90° through the whole specimen in the RL orientation. The crack cannot stay within one TL plane but has to "jump" from one annual ring to the other (Fig. 13). More or less rough fracture surfaces are therefore formed with higher and lower edges so that the cracking resistance depends on this fracture morphology to a high degree. Similarly, structural inhomogeneities result in different crack growth paths in the TL orientation. Thus intrinsic influences of orientation, drying temperature, etc. on fracture energy may be confounded by this effect to a large extent.

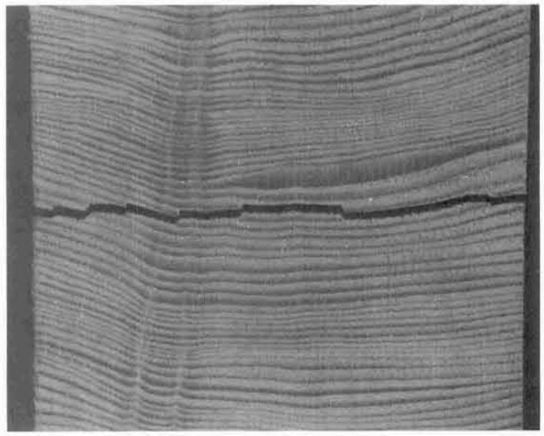

Fig. 13. Fracture path in the RL orientation: crack does not propagate within one annual ring but changes its path in order to keep its perpendicular direction towards the acting force.

This effect could explain, for example, the different G_f values of the winter cut after high-temperature drying in the RL orientation for the north and south sides (Fig. 4). Careful evaluation showed that the fracture surfaces of the specimens from the south side were flatter and more homogeneous than from the north side. Reasons for that are so far unknown. It is assumed, however, that the lower fracture energy values after high-temperature drying as seen in Fig. 4 for the south side of the winter cut are the more typical values, which are not confounded by an extremely rough crack path. In view of this result, the following tendencies for the drying temperature influence on fracture energy are found for the RL orientation:

1. The felling time (winter and summer) has no remarkable influence on the fracture energy in all drying procedures. However, this result may not be typical as there had been an untypically warm period of 3 weeks before felling time.
2. The fracture energy values (G_f) are not notably influenced by the compass orientation of the trees, i.e., the values are similar for the north and south sides of each tree.
3. The G_f values decrease with increasing drying temperature (in the range of 20–110 C), at least for the RL orientation in all cases (winter and summer felling, north and south side).

The No. 1 and No. 2 results are similar for the TL orientation. However, the influence of the drying temperature is not so clear. According to Fig. 5, it seems that high-temperature drying reveals the highest G_f values in comparison with lower drying temperatures. The authors believe that this is not a typical result but a consequence of the above-mentioned phenomenon of differing crack paths. Especially in the TL orientation, the crack paths may be extremely different, as has been observed from the resulting fracture surfaces: they are characterized partly by large edges and thus very rough fracture surfaces. Therefore, it is assumed that the data points of Fig. 5 vary within the inherent scatterband and do not really show a trend of the drying temperature.

The fracture toughness, K_{IC}, may be considered as a parameter that characterizes the strength properties of the tested material containing a specific macroscopic crack (15.5 mm in this study). Besides less scatter of the measurements (no influence by different crack propagation paths) in comparison with the G_f measurements, the results of this paper reveal essentially similar tendencies as to the influences of drying procedure, felling time, and compass orientation.

In addition, one more detail can be recognized with the K_{IC} results: Scattering of the values is more pronounced for the specimens from trees cut in summer than from wood cut in winter. This result is in accordance with the Hinterstoisser et al. (1992) findings, which showed a more inhomogeneous distribution of water extractable carbohydrates and reducing substances across the cross section of trees cut in summer in comparison with trees cut in winter.

At first sight, one might think that K_{IC} is more useful to characterize the loading capability of wood than G_f, because of less scatter of the results. For practical application, however, the life time of some wood components does not depend only on the time to initiate a crack but also on the crack propagation properties. Crack propagation and crack initiation are best characterized by the fracture energy, G_f, whereas K_{IC} only gives information on crack initiation.

In order to obtain more conclusive answers from G_f measurements, two ways are possible in principle. One is to increase the number of tests. This possibility, however, will be too expensive in most cases. The second possibility is to reduce the specimen size so that orientation influences, which result in scatter owing to geometrical (orientation) effects, are minimized. Therefore, the authors have performed studies on the specimen size effect. The results are presented in another work (Stanzl-Tschegg et al. 1994).

The results of this study—essentially similar tendencies of drying temperature influence on K_{IC} and G_f values in such an anisotropic material like wood—are surprising. More research is necessary to understand this result and to find out if it is true for other wood species as well.

SUMMARY AND CONCLUSIONS

The specific fracture energy, G_f, is the most useful parameter to characterize the fracture behavior of wood, as not only crack initiation but also crack propagation properties and nonlinear effects like crack closure owing to fiber bridging are considered by the measuring procedure.

Scatter of the results of this study is rather high, but this can be reduced in future studies by optimizing the specimen shape so that secondary orientation influences are minimized.

High-temperature (100–110 C) drying renders the lowest specific fracture energy (G_f) and fracture toughness (K_{IC}) values in comparison with 20 C fresh air, 50–60 C (kiln) drying and prefreezing (−20 C) + air-drying. Prefreezing to −20 C before air-drying provides similar values as 20 C and similar or little higher values as 50 C drying.

Effects of felling time (summer and winter) and compass orientation within the tree (north and south side) could not be detected unambiguously. Owing to high scatter of the results, it cannot be decided whether minor influences are present or not. The K_{IC} values of wood cut in summer, together with results of chemical investigations by Hinterstoisser et al. (1992), point to some effect of felling time on fracture toughness and fracture energy.

SEM observations of microstructural cracks as a result of the drying procedure may partly explain the G_f and K_{IC} results.

ACKNOWLEDGMENTS

The authors thank Mr. König for his experimental work and Mrs. Shao Qing for the SEM photographs. We also thank Prof. Führer and Dr. Wegensteiner for permission to use their SEM. We gratefully acknowledge funding by the Wiener Handelskammer (Bodenkulturpreis) and the Fonds zur Förderung der wissenschaftlichen Forschung, Wien (Austrian Science Foundation).

REFERENCES

Barrett, J. D. 1976. Effect of crack-front width on fracture toughness of Douglas-fir. Eng. Fract. Mech. 8(4): 711–717.

———, and R. O. Foschi. 1977. Mode II stress-intensity factors for cracked wood beams. Eng. Fract. Mech. 9: 371–378.

Boatright, S. W. J., and G. G. Garrett. 1983. The effect of microstructure and stress state on the fracture behaviour of wood. J. Mater. Sci. 18:2181–2199.

Boström, L. 1992. Method for determination of the softening behaviour of wood and the applicability of a nonlinear fracture mechanics model. Universitatis Gothorum, CODEN: LUTVOG (TVBM-1012) 1–132.

DIN 52 182. 1976. Prüfung von Holz: Bestimmung der Rohdichte (Testing of wood: Determination of density). Deutsches Institut für Normung e.v., Berlin.

Ewing, P. D., and J. G. Williams. 1979. Thickness and moisture content effect in the fracture toughness of Scots pine. J. Mater. Sci. 14:2959–2966.

Hillerborg, A. 1991. Application of the fictitious crack model to different types of materials. Intl. J. Fract. 51: 95–102.

Hinterstoisser, B., J. Weingärtner, and W. Praznik. 1992. Influence of wood drying processes on the carbohydrate matrix of wood of *Picea abies*. *In* M. Vanek, ed. Proceedings of the 3rd International Conference on Wood Drying, Vienna, Austria.

Kayihan, F., J. A. Johnson, and W. R. Smith, eds. 1989. Upgrading wood quality through drying technology. Proceedings IUFRO Wood Drying Symposium, Seattle, WA.

Navi, P. 1992. Crack stability study of wood in RL-LR system. *In* COST 508, Workshop on Fracture Mechanics in Wooden Materials, Bordeaux, France.

Patton-Mallory, M., and S. M. Cramer. 1987. Fracture mechanics: A tool for predicting wood component strength. Forest Prod. J. 37(7/8):39–47.

Petersson, H. 1992. Analysis of fracture propagation. *In* COST 508, Workshop on Fracture Mechanics in Wooden Materials, Bordeaux, France.

Petterson, R. W., and J. Bodig. 1983. Prediction of fracture toughness of conifers. Wood Fiber Sci. 15(4): 302–316.

Porter, A. W. 1964. On the mechanics of fracture in wood. Forest Prod. J. 14(8):325–331.

Schniewind, A. P., T. Ohgama, T. Aoki, and T. Yamada. 1982. Effect of specific gravity, moisture content, and temperature on fracture toughness of wood. Wood Sci. 15(2):101–109.

———, and R. A. Pozniak. 1971. On the fracture toughness of Douglas fir wood. Eng. Fract. Mech. 2:223–233.

Stanzl-Tschegg, S. E., D. M. Tan, and E. K. Tschegg. 1994. New splitting test method for wood—Development and experiences. Wood Sci. Technol. (in press).

Teischinger, A. 1991. Der Einfluss des Trocknungsverfahrens auf ausgewählte Holzkennwerte, Teil 1. Holzforsch. Holzverwert. 43(1):20–22.

———. 1992. Der Einfluss des Trocknungsverfahrens auf ausgewählte Holzkennwerte, Teil 2. Holzforsch. Holzverwert. 44(5):83–86.

Triboulot, P., P. Jodin, and G. Pluvinage. 1984. Validity of fracture mechanics concepts applied to wood by finite element calculation. Wood Sci. Technol. 18: 51–58.

Tschegg, E. K. 1986. Equipment and appropriate specimen shape for tests to measure fracture values (in German). Austrian patent AT-390328, 1986.

———, and S. E. Stanzl. 1991. Adhesive power of bonded concrete. Pages 809–816 *in* G. M. van Mier, J. G. Rots, and A. Bakker, eds. Fracture processes in concrete, rock, and ceramics. E & F SPON.

VALENTIN, G., AND G. ADJANOHOUN. 1992. Applicability of classical isotropic fracture mechanics specimens to wood propagation studies. Mater. Struct. 25:3–13.

WELLING, J., AND C. SALES. 1992. EDG-recommendation on assessment of drying quality. *In* M. Vanek, ed. Proceedings of 3rd IUFRO International Conference on Wood Drying, Vienna, Austria.